

# 000 001 002 003 004 Markovian Transformers for Informative Language Mod- eling

005  
006 Anonymous authors  
007 Paper under double-blind review

## 008 009 Abstract 010

011 Chain-of-Thought (CoT) reasoning often fails to faithfully reflect a lan-  
012 guage model’s underlying decision process. We address this by introducing  
013 a Markovian language model framework that can be understood as a rea-  
014 soning autoencoder: it creates a text-based bottleneck where CoT serves  
015 as an intermediate representation, forcing the model to compress essential  
016 reasoning into interpretable text before making predictions. We train this  
017 system with a GRPO-style policy gradient algorithm using parallel sam-  
018 pling, a frozen baseline CoT’, within-batch standardized advantages, and  
019 actor-reward (chain-rule) gradients. On QA tasks, Markovian training re-  
020 covers most of the gains of a non-Markovian GRPO variant while forcing  
021 the model to answer from the CoT alone (e.g., GSM8K: 19.6% → 57.1%;  
022 ARC-Challenge: 36.1% → 79.9%; on average only ≈3–4 pp below a non-  
023 Markovian upper bound). Perturbation analyses across types and severi-  
024 ties show that Markovian models incur systematically larger log-probability  
025 drops under CoT corruption than matched Non-Markovian baselines, indi-  
026 cating stronger causal reliance on the CoT. Cross-model evaluation confirms  
027 that learned CoTs generalize across architectures, suggesting they capture  
028 transferable reasoning patterns rather than model-specific artifacts.

## 029 030 1 Introduction 031

032 The rapid advancement of language models (LMs) has led to impressive performance on  
033 complex cognitive tasks (Brown et al., 2020). Yet it is often unclear why an LM arrives at  
034 a particular conclusion (Lamparth & Reuel, 2023; Burns et al., 2023; Gurnee & Tegmark,  
035 2024), causing issues in high-stakes applications (Grabb et al., 2024; Lamparth et al., 2024;  
036 Rivera et al., 2024). Traditional interpretability methods analyze hidden activations or  
037 attention patterns to extract “explanations” (Geiger et al., 2022; Geva et al., 2022; Meng  
038 et al., 2022; Casper et al., 2023; Wang et al., 2022; Lamparth & Reuel, 2023; Nanda et al.,  
039 2023). Modern LMs, however, already generate coherent text: we might hope prompting  
040 the model to articulate its reasoning (“Chain-of-Thought” or CoT) (Nye et al., 2022; Wei  
041 et al., 2022) would yield a faithful record of its thought process.

042 Unfortunately, CoT explanations can be unfaithful. For example, Turpin et al. (2023) show  
043 that spurious in-context biases often remain hidden in the CoT, and Lanham et al. (2023)  
044 find that altering CoT text may not affect the final answer. Such observations indicate that  
045 standard CoTs are not “load-bearing.”

046 In this work, we take a pragmatic approach to interpretability, focusing on informativeness  
047 over full faithfulness. Rather than insisting the CoT mirrors the model’s entire internal  
048 process, we require that the CoT alone suffices to produce the final answer. In other words,  
049 if we remove the original prompt and rely only on the CoT, the model should still reach the  
050 correct output. This makes the CoT causally essential and fragile: changing it necessarily  
051 alters the prediction.

052 What distinguishes our approach is the clear distinction between the model relying on its  
053 CoT versus generating more informative CoTs. While traditional approaches train models  
to generate better-quality CoTs, they don’t fundamentally change how the model uses them.

Our Markovian framework, by contrast, forces the model to process information through the CoT bottleneck, making the CoT not just informative but causally load-bearing for prediction.

For instance, Llama’s CoT on arithmetic tasks changed dramatically after training. Before training, it simply listed all numbers and their (incorrect) sum (e.g., “Sum =  $76 + 90 + 92 + \dots = 2314$ ”). After training, it performed correct step-by-step calculations (e.g., “calculate  $6 + 89 = 95$ ; Next, calculate  $95 + 38 = 133\dots$ ”), breaking the task into manageable steps that can be verified independently and enabling accurate answer prediction even when the original question is removed.

**Recipient-Specific Compression.** A key insight is that an informative CoT can also serve as a recipient-specific compression of the model’s hidden knowledge: it distills the essential reasoning into text that another recipient (e.g. a different model or a human) can use to predict the same outcome. Our experiments confirm that the learned CoTs generalize across interpreters, suggesting that these textual explanations genuinely encode transferable problem-solving steps rather than model-specific quirks (Section 5.4).

## Contributions.

1. We introduce a Markovian language model framework that structurally enforces CoT generation to be causally essential, together with a GRPO-style training recipe (parallel sampling, frozen CoT baseline, actor-reward gradients) that optimizes this objective through a discrete text bottleneck.
2. We apply this framework to arithmetic problems (Mistral 7B) and standard QA datasets (GSM8K, MMLU, SVAMP, ARC-Challenge; Llama 3.1 8B), observing large absolute gains over the base model (e.g., GSM8K 19.6%  $\rightarrow$  57.1%, ARC-Challenge 36.1%  $\rightarrow$  79.9%) while remaining within  $\approx$ 3–4 percentage points of a Non-Markovian GRPO variant that can still see the question during answer prediction.
3. We show through systematic perturbation analyses on Wikipedia continuation and multiple QA datasets that Markovian training produces consistently higher sensitivity to CoT perturbations compared to matched Non-Markovian baselines (Tables 1 and 3), indicating that the learned CoTs are more causally load-bearing.
4. We demonstrate cross-model transfer: CoTs trained on one model (Llama 3.1 8B) remain informative for diverse other models (Mistral, Phi, Qwen, GPT-2) on GSM8K and Wikipedia. This underscores the CoT’s recipient-specific informativeness and suggests it captures a shared reasoning strategy rather than model-specific artifacts.

Section 2 reviews related work, Section 3 details our Markovian framework, and Section 4 describes the RL training. Section 5 presents empirical results, and Section 6 discusses limitations and future directions.

## 2 Related Work

Prior work shows that CoT prompting can boost performance on reasoning tasks (Wei et al., 2022; Nye et al., 2022). Whereas typical CoT prompting methods do not alter a pre-trained model’s parameters, some prior approaches do fine-tune the model for CoT generation (Zelikman et al., 2022; 2024; DeepSeek-AI et al., 2025). Our work differs by removing the original question or passage from the answer-prediction context, which enforces a stronger causal reliance on the CoT.

Regarding faithfulness vs. interpretability, some authors discuss how a CoT may fail to reflect the true reason the LM arrived at its answer (Lanham et al., 2023; Turpin et al., 2023), since small changes in the CoT do not necessarily change the final prediction. Zhou et al. (2023) analyze CoT through an information-theoretic lens, finding that CoT can serve as a communication channel between different parts of a model. We build on these insights by training the model to rely on this channel exclusively.

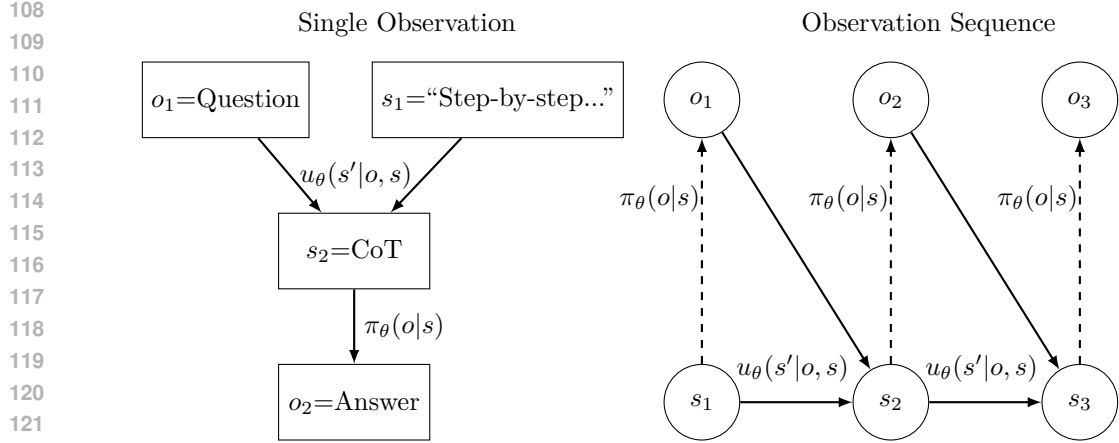


Figure 1: Markovian training as a reasoning autoencoder. Left: Single time-step process from Question to CoT to Answer, creating a text-based bottleneck where the CoT must capture all information needed for answer prediction. Right: Causal structure showing the generation of states from observations and previous states using the state update function  $u_{\theta}(s'|o, s)$ , and the prediction of observations from states using the policy  $\pi_{\theta}(o|s)$ . This architecture forces reasoning through an interpretable text bottleneck, but prevents direct backpropagation, necessitating RL-based gradient estimation.

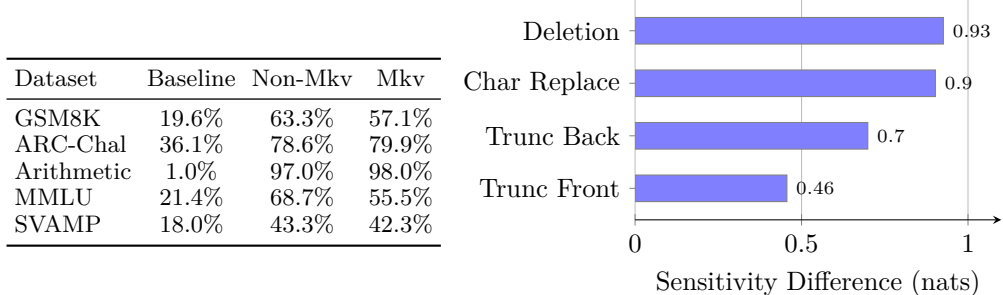


Figure 2: (a) Accuracy comparison. Markovian models (Mkv) maintain competitive performance with Non-Markovian upper bounds despite the strict information bottleneck. (b) Wiki perturbation sensitivity (positive = Mkv more fragile). Markovian models are significantly more sensitive to CoT corruption (higher  $\Delta \ln P$ ), confirming the CoT is causally load-bearing.

Architecturally, our Markovian LM shares structural similarities with state space models like RNNs (Rumelhart et al., 1986), S4 (Gu et al., 2022), and Mamba (Gu & Dao, 2024), though with a key difference: MLMs have probabilistic state transitions to model token sampling, which necessitates gradient estimation methods such as policy gradient (Sutton et al., 1999) rather than direct backpropagation. This probabilistic structure also resembles Kalman filters (Å ström, 1965), Deep Variational Bayes Filters (Karl et al., 2017), Deep Kalman Filters (Krishnan et al., 2015), and Variational Recurrent Neural Networks (VRNN) (Chung et al., 2015), though we use categorical rather than Gaussian distributions for interpretable text generation. Other fine-tuned reasoning models mentioned above (R1, STar, and QuietSTar) have similar structure but allow seeing the full context before generating state/reasoning tokens, whereas our approach enforces a strict information bottleneck through the state.

Lyu et al. (2023) also consider restricting the model’s ability to see the original input while generating the final answer. Their approach, however, involves rewriting the question in a structured formal language or code that is then executed. Our approach uses natural language for the reasoning state to preserve interpretability across diverse tasks.

---

162    

### 3 Markovian Language Models and Informativeness

163

164    Here we provide our formalism for Markovian Language Models (MLMs) and define infor-
165    mative ness, which we use as a training objective within our novel structural framework.
166

167    

#### 3.1 Markovian Language Models (MLM)

168

169    A traditional LM can attend to the entire context when predicting the next token. This
170    makes it possible for an LM to disregard the CoT or only partially rely on it. We impose a
171    stricter, Markovian structure<sup>1</sup>:

172    Definition 3.1 (Markovian LM). A Markovian Language Model is a tuple  $M =$ 
173     $(\mathcal{O}, \mathcal{S}, \pi, u, s_1)$ , where
174

- 175    •
- $\mathcal{O}$
- is a set of observations (e.g., questions and answers in a QA task),
176    •
- $\mathcal{S}$
- is a set of states (e.g., CoT reasoning text),
177    •
- $\pi : \mathcal{S} \rightarrow \Delta(\mathcal{O})$
- is a policy that predicts the next observation from the state alone,
178    •
- $u : \mathcal{O} \times \mathcal{S} \rightarrow \Delta(\mathcal{S})$
- is a state update function (produces CoT from question and
179    initial prompt),
180    •
- $s_1 \in \mathcal{S}$
- is an initial state (starting CoT prompt).
181

182    For example, in a math reasoning task,  $o_1 \in \mathcal{O}$  might be a question,  $s_1 \in \mathcal{S}$  is an initial
183    CoT prompt like ‘‘Let’s solve this step-by-step:’’,  $s_2 \in \mathcal{S}$  is the generated reasoning chain,
184    and  $o_2 \in \mathcal{O}$  is the answer. The key idea is that  $\pi$  can only see the CoT state  $s_2$  when
185    predicting  $o_2$ , forcing the CoT to contain all needed information. Intuitively,  $\pi$  is the next-
186    token predictor, and  $u$  chooses how to produce the CoT from the latest observation and
187    prior state. In our experiments,  $\pi$  and  $u$  are the same underlying transformer; we denote
188    the trainable pair by  $(u_\theta, \pi_\theta)$  and the frozen baseline pair by  $(u', \pi')$ .
189

190    

#### 3.2 Data-Generating Distribution and Reward

191    Let  $P$  be the distribution over observations  $x_1, x_2, \dots, x_T \in \mathcal{O}$ . A trajectory  $\tau$  is generated
192    by:

193    
$$s_{t+1} \sim u_\theta(s_t, x_t), \quad x_{t+1} \sim P(x_{t+1} | x_{\leq t}),$$

194    with  $s_1$  a fixed initial prompt. We define the reward for a trajectory  $\tau$  as:

195    
$$R_\theta(\tau) = \sum_{t=1}^T [\ln \pi_\theta(x_t | s_t) - \ln \pi'(x_t | s'_t)],$$

196    where  $s'_t$  is generated by a baseline update function  $u'$ , e.g., the untrained model, and  $\pi'$  is
197    the corresponding frozen baseline policy. In words,  $R_\theta(\tau)$  measures how much more likely
198    the correct observation  $x_t$  is under the trained state  $s_t$  (scored by  $\pi_\theta$ ) compared to the
199    baseline state  $s'_t$  (scored by  $\pi'$ ).
200

201    

#### 3.3 Informativeness Objective

202    Conceptually, we aim to ensure that the CoT state serves as a critical bottleneck for in-
203    formation flow, making it causally essential for predictions. Formalizing this within our
204    Markovian framework, we define:

205    
$$J(\theta) = \mathbb{E}_{\tau \sim P, u_\theta, u'} [R_\theta(\tau)],$$

206    

---

207    <sup>1</sup>This structure can be viewed as a stochastic variant of a Moore machine where both the
208    transition function ( $u$ ) and output function ( $\pi$ ) are probabilistic, and the input and output alphabets
209    are identical ( $\mathcal{O}$ ). Alternatively, an MLM can be formalized as an F-coalgebra where  $F(S) = P(O)$ 
210     $\times P(S)^O$ , with  $P$  representing probability distributions.
211

216 where  $\theta$  parameterizes the trainable pair. Maximizing  $J(\theta)$  ensures that the update function  
 217  $u_\theta$  produces states  $s_t$  that are informative to  $\pi_\theta$  about future observations (relative to the  
 218 baseline  $u'$  and  $\pi'$ ), thereby enforcing the CoT’s role as a load-bearing component. We  
 219 optimize  $J(\theta)$  with policy-gradient methods (including our GRPO-style update), sampling  
 220 observations from  $P$  and states from  $u_\theta$  and  $u'$ .

## 222 4 Methods

### 224 4.1 Implementation as Question-Answer Pairs

226 In many tasks like math problem solving, we have  $T = 2$  observations (question and answer)  
 227 and implement the abstract MLM with a fixed maximum length for the CoT state. Let  $\mathcal{V}$   
 228 be a token vocabulary. We set  $\mathcal{O} = \mathcal{V}^N$  and  $\mathcal{S} = \mathcal{V}^K$  for some  $N, K \in \mathbb{N}$ , where  $K$  is the  
 229 maximum tokens in the CoT. Note that while we limit the state to a maximum of  $K$  tokens  
 230 for implementation, we do not enforce fixed-length observations.

231 Our conceptual arguments rely on  $K < N$ , as otherwise the model could simply write the  
 232 predicted observation into the state. We satisfy this in our Wikipedia experiments (Sec 5.2),  
 233 and for other experiments we find empirically that the model does not learn this undesirable  
 234 behavior due to the difficulty of predicting the answer directly without any CoT.

235 In this setting, we denote our states as  $s_1 = \text{CoT}_{\text{init}}$  and  $s_2 = \text{CoT}$ , where  $\text{CoT}_{\text{init}}$  is a  
 236 task-specific prompt<sup>2</sup>. With pre-trained LM  $\mathcal{L}$ , we can implement our update function  $u$   
 237 and policy  $\pi$  using:

$$\begin{aligned} \ln u_\theta(s_2 = \text{CoT} \mid q, s_1 = \text{CoT}_{\text{init}}) &= \sum_{i=1}^K \ln \mathcal{L}_\theta(\text{concat}(q, \text{CoT}_{\text{init}}, \text{CoT}_{<i}))[\text{CoT}_i], \\ \ln \pi_\theta(\text{ans} \mid \text{CoT}) &:= \sum_{i=1}^N \ln \mathcal{L}_\theta(\text{concat}(\text{CoT}, \text{ans}_{<i}))[\text{ans}_i]. \end{aligned}$$

244 Compression viewpoint. Our ”CoT as compression” narrative applies most directly to con-  
 245 tinuation tasks (e.g., Wikipedia), where the content to be predicted is longer than the CoT,  
 246 forcing the model to compress salient context into a short textual bottleneck. For QA tasks,  
 247 the answer is typically shorter than the CoT; there we emphasize the CoT’s sufficiency and  
 248 fragility rather than literal compression, and use QA as evidence that the training method  
 249 generalizes across task types.

250 Crucially, we do not allow the answer generation to attend back to the question  $q$  directly;  
 251 the question is replaced by the CoT. For each question  $q$ , we generate the baseline state  $s'_2$   
 252 (which we denote as  $\text{CoT}'$  in this setting) by prompting the unmodified pre-trained model  $u'$   
 253 with  $q$  plus an initial instruction (e.g., ’Think step-by-step...’), and recording its raw output.

254 Our reward is:

$$R_\theta = \ln \pi_\theta(\text{ans} \mid \text{CoT}) - \ln \pi'(\text{ans} \mid \text{CoT}').$$

### 257 4.2 Policy Gradient with GRPO-Style Baseline

259 Markovian training can be viewed as the reasoning autoencoder introduced in Section 3,  
 260 where the CoT is a discrete text bottleneck between question and answer. This bottleneck  
 261 blocks direct backpropagation through token sampling, so we rely on reinforcement learning  
 262 techniques for gradient estimation.

#### 264 4.2.1 Actor Reward Gradients: An Important Innovation

266 Our approach differs from standard policy gradient setups, where the reward  $R(\tau)$  is treated  
 267 as independent of the policy parameters (or any  $\theta$ -dependence is stopped by gradient de-  
 268 attachment). Here the same transformer with weights  $\theta$  defines both the sampling distribution

269 <sup>2</sup>The exact prompt template varies by task type, with each template specifying the task objective,  
 allowed CoT length, and an invitation to reason strategically. Full templates are provided in Sec A.

270  $P_\theta(\tau)$  via  $u_\theta$  and the reward term  $\ln \pi_\theta(\text{ans} | \text{CoT})$ , and we explicitly backpropagate through  
 271 this reward in addition to the usual REINFORCE term.

272 In classical policy gradient, the reward  $R(\tau)$  is independent of the policy parameters, leading  
 273 to the standard REINFORCE gradient:  
 274

$$275 \nabla_\theta \mathbb{E}_{\tau \sim P_\theta}[R(\tau)] = \mathbb{E}_{\tau \sim P_\theta}[R(\tau) \cdot \nabla_\theta \ln P_\theta(\tau)]$$

276 However, in our case, the reward is a function of the same parameters via the actor term:  
 277  $R_\theta(\tau) = \ln \pi_\theta(\text{ans} | \text{CoT}) - \ln \pi'(\text{ans} | \text{CoT}')$ . Applying the chain rule:  
 278

$$279 \nabla_\theta \mathbb{E}_{\tau \sim P_\theta}[R_\theta(\tau)] = \mathbb{E}_{\tau \sim P_\theta}[R_\theta(\tau) \nabla_\theta \ln P_\theta(\tau) + \nabla_\theta R_\theta(\tau)].$$

280 This yields two terms: the standard policy gradient ( $R_\theta(\tau) \cdot \nabla_\theta \ln P_\theta(\tau)$ ) and the direct  
 281 reward gradient ( $\nabla_\theta R_\theta(\tau)$ ). We include both terms with equal weight in our implementation.  
 282

#### 283 4.2.2 GRPO-Style Baseline with Local Subtraction

285 We implement a policy gradient algorithm inspired by Group Relative Policy Optimization  
 286 (GRPO), originally introduced by Shao et al. Shao et al. (2024) in DeepSeek-Math. GRPO  
 287 eliminates the critic model from PPO by using group-based advantage estimation, where  
 288 multiple responses to the same query provide relative baselines for each other.

289 However, we add an additional baseline subtraction step before applying GRPO’s batch  
 290 averaging. We first compute a local baseline using the frozen reference model  $u'$ , then apply  
 291 GRPO-style standardization within each batch.  
 292

#### 293 4.2.3 Parallel Sampling Strategy

294 We employ parallel sampling (inspired by GRPO): each training batch contains  $B$  copies of  
 295 the same question-answer pair  $(q, a)$ . The trainable model  $u_\theta$  generates diverse reasoning  
 296 chains  $\{\text{CoT}_1, \text{CoT}_2, \dots, \text{CoT}_B\}$  for the identical input through stochastic sampling.  
 297

298 Additionally, we introduce a frozen baseline from the reasoning autoencoder: the unmodified  
 299 model  $u'$  generates a single reference CoT’ that provides a local baseline before applying  
 300 GRPO-style batch averaging. This frozen baseline represents the “encoder” component of  
 301 our reasoning autoencoder—capturing the model’s initial reasoning ability before training.  
 302 The frozen baseline CoT’ is not part of the original GRPO algorithm—it is our contribution  
 303 to provide a more stable reference point.  
 304

This approach provides several advantages:

- 305 • Reasoning bottleneck: The CoT’ baseline establishes the initial encoding capacity  
 306 of the reasoning autoencoder
- 307 • Local baseline: The frozen CoT’ provides a consistent reference for measuring in-  
 308 formativeness improvement
- 309 • Computational efficiency: Baseline reasoning and answer evaluation are computed  
 310 once and replicated
- 311 • Stable variance estimation: All samples share the same ground truth, enabling  
 312 robust within-batch standardization

#### 314 4.2.4 Implementation: Two-Term Loss Function

316 Our implementation combines both gradient terms from the chain rule derivation above.  
 317 The loss function includes:

$$318 \mathcal{L} = \mathcal{L}_{\text{PG}} + \mathcal{L}_{\text{AR}}, \quad \mathcal{L}_{\text{PG}} = -\ln u_\theta(\text{CoT} | q, \text{CoT}_{\text{init}}) \cdot A^{\text{detach}}, \quad \mathcal{L}_{\text{AR}} = -A.$$

319 where  $A$  is the standardized advantage (after local baseline subtraction and GRPO-style  
 320 batch averaging) and  $A^{\text{detach}}$  blocks gradients to isolate the policy gradient term.  
 321

322 The first term  $\mathcal{L}_{\text{PG}}$  corresponds to the standard REINFORCE gradient  $A_\theta(\tau) \cdot \nabla_\theta \ln P_\theta(\tau)$ ,  
 323 while the second term  $\mathcal{L}_{\text{AR}}$  corresponds to the direct advantage gradient  $\nabla_\theta A_\theta(\tau)$ . This  
 enables simultaneous optimization of CoT generation and answer prediction.

---

324      Algorithm 1 Markovian Training with GRPO-Style Batch Baseline  
 325  
 326      1: Given dataset  $P$  of  $(q, a)$ , trainable actor  $(u_\theta, \pi_\theta)$ , frozen baseline  $(u', \pi')$ , batch size  $B$   
 327      2: for each training batch do  
 328        3:     Sample  $(q, a) \sim P$   
 329        4:     Sample  $\text{CoT}_i \sim u_\theta(\cdot | q, \text{CoT}_{\text{init}})$  for  $i = 1..B$  (stochastic parallel sampling)  
 330        5:     Sample baseline  $\text{CoT}' \sim u'(\cdot | q, \text{CoT}_{\text{init}})$  (once per batch)  
 331        6:     Compute actor answer log-probs  $r_i = \ln \pi_\theta(a | \text{CoT}_i)$   
 332        7:     Compute baseline log-prob  $b = \ln \pi'(a | \text{CoT}')$   
 333        8:     Normalized rewards  $R_i = r_i - b$ ; standardize within-batch:  $A_i = \frac{R_i - \mu}{\sigma + \epsilon}$   
 334        9:     Policy gradient loss:  $\ell_i^{\text{PG}} = -\ln u_\theta(\text{CoT}_i | q, \text{CoT}_{\text{init}}) \cdot A_i^{\text{detach}}$   
 335        10:   Actor-reward gradient:  $\ell_i^{\text{AR}} = -A_i$   
 336        11:   KL penalty:  $\ell_i^{\text{KL}} = 0.1 D_{KL}(u_\theta(\cdot | q) \| u'(\cdot | q))$   
 337        12:   Total loss:  $\ell_i = \ell_i^{\text{PG}} + \ell_i^{\text{AR}} + \ell_i^{\text{KL}}$ ; update  $\theta$  with  $\frac{1}{B} \sum_i \ell_i$   
 338        13: end for

---

340  
 341      4.2.5 Within-Batch Advantage Standardization

342  
 343      Instead of historical exponential moving averages, we standardize advantages within each  
 344      batch so that they have zero mean and unit variance (Algorithm 1), which stabilizes training  
 345      regardless of the absolute reward scale.

346  
 347      5 Experiments

348  
 349      We evaluate in two regimes: (i) continuation (Wikipedia), where CoT tokens act as a lossy  
 350      compression of longer context, and (ii) question–answer datasets (GSM8K, MMLU, SVAMP,  
 351      AQuA, ARC, Arithmetic), which validate the general-purpose efficacy of Markovian training  
 352      even when the “compression” story is not literal.

353  
 354      5.1 Question–Answer Tasks (GSM8K, MMLU, SVAMP, ARC, Arithmetic)

355  
 356      We evaluate on standard QA-style datasets (GSM8K (Cobbe et al., 2021),  
 357      MMLU (Hendrycks et al., 2020), SVAMP (Patel et al., 2021), ARC Challenge (Clark et al.,  
 358      2018), and our non-standard multi-step addition task. All QA experiments use the same  
 359      optimization: GRPO-style parallel sampling with within-batch standardization and the  
 360      chain-rule reward (policy-gradient plus actor-reward gradient), with task-specific default  
 361      CoT lengths. For arithmetic, each problem has fifteen random terms in  $[1, 99]$ ; the model  
 362      learns to produce step-wise reasoning and achieves  $> 99\%$  verbatim-correct answers at  $T=0$ .

363  
 364      CoT length defaults. Unless otherwise specified, we use: GSM8K 100, Arithmetic 150,  
 365      Arithmetic-Negative 150, MMLU 150. See §4 for objective details.

366  
 367      5.2 Wikipedia Continuation

368  
 369      For Wikipedia continuation (Foundation, 2024), we condition on the first 200 tokens and  
 370      predict the next 100 tokens, allowing 50 tokens of CoT. Training uses the same GRPO with  
 371      chain-rule reward as in QA. We observe improvements consistent with increased CoT infor-  
 372      mativity (cf. Fig. 2), and §5.3 shows stronger perturbation sensitivity under Markovian  
 373      training.

374  
 375      5.3 Markovian vs Non-Markovian Perturbation Sensitivity

376  
 377      To provide systematic evidence for the theoretical advantages of Markovian training, we  
 378      conduct comprehensive perturbation sensitivity comparisons between Markovian and Non-  
 379      Markovian model pairs. The Non-Markovian models are trained using the same hyperpa-  
 380      rameters, only differing in that the reward is  $\pi_{\theta'}(\text{ans} | q, \text{CoT})$  instead of  $\pi_\theta(\text{ans} | \text{CoT})$ .

Severity	Char Replace	Delete	Digit Replace	Truncate Back	Truncate Front	Row Mean
20%	+0.457	+0.459	+0.016	+0.254	-0.009	+0.235
40%	+0.849	+0.836	+0.025	+0.368	+0.121	+0.440
60%	+1.042	+1.002	+0.035	+0.596	+0.284	+0.592
80%	+1.079	+1.069	+0.038	+1.020	+0.622	+0.766
100%	+1.084	+1.263	+0.039	+1.258	+1.262	+0.981
Column Mean	+0.902	+0.926	+0.030	+0.699	+0.456	+0.603

Table 1: Perturbation fragility on Wikipedia continuation. Entries report  $\Delta \ln P = (\text{Markovian drop} - \text{Non-Markovian drop})$ , where the Markovian drop is  $\ln \pi_\theta(\text{ans} | \text{CoT}^M) - \ln \pi_\theta(\text{ans} | \widetilde{\text{CoT}}^M)$  and the Non-Markovian drop is  $\ln \pi_{\theta'}(\text{ans} | q, \text{CoT}^{NM}) - \ln \pi_{\theta'}(\text{ans} | q, \widetilde{\text{CoT}}^{NM})$ . Here  $\theta$  denotes the Markovian checkpoint that must answer from the CoT alone, while  $\theta'$  is the Non-Markovian checkpoint that additionally conditions on the question  $q$ . Values are averaged over 1,024 held-out examples per perturbation type and severity. Positive values mean the Markovian actor relies more on intact CoTs. Row means summarize severity-wise fragility, while the column-mean row highlights which perturbation families disrupt Markovian reasoning the most (delete and truncate operations produce the largest gaps).

This analysis directly evaluates whether the structural constraints in Markovian training lead to measurably different robustness properties during training.

### 5.3.1 Experimental Design

We maintain two independently trained checkpoints: the Markovian weights  $\theta$ , which are always asked to score ans conditioned solely on the actor’s CoT, and the Non-Markovian weights  $\theta'$ , which additionally attend to the original question  $q$  during both training and evaluation. For each held-out  $(q, \text{ans})$  pair we run both models on the same data point, sampling fresh reasoning traces  $\text{CoT}^M \sim u_\theta(\cdot | q)$  and  $\text{CoT}^{NM} \sim u_{\theta'}(\cdot | q)$ . We then perturb each CoT independently, producing  $\widetilde{\text{CoT}}^M$  and  $\widetilde{\text{CoT}}^{NM}$ , and ask the corresponding model (using its own weights and visibility constraints) to score the answer with the original versus perturbed CoT. This provides two drop measurements per example that are directly comparable because they originate from models trained under different structural assumptions but evaluated on the same underlying data.

We test four perturbation types at five severities (20%, 40%, 60%, 80%, 100%):

- Delete: Random token deletion from CoT reasoning
- Digit Replace: Random replacement of numeric characters within tokens
- Truncate Front: Removal of tokens from CoT beginning
- Truncate Back: Removal of tokens from CoT end
- Character Replace: Random character substitution within tokens

The sensitivity measure matches the implementation:

$$\text{Effect}_M = \ln \pi_\theta(\text{ans} | \text{CoT}^M) - \ln \pi_\theta(\text{ans} | \widetilde{\text{CoT}}^M) \quad (1)$$

$$\text{Effect}_{NM} = \ln \pi_{\theta'}(\text{ans} | q, \text{CoT}^{NM}) - \ln \pi_{\theta'}(\text{ans} | q, \widetilde{\text{CoT}}^{NM}) \quad (2)$$

$$\text{Difference} = \text{Effect}_M - \text{Effect}_{NM} \quad (3)$$

Positive differences indicate greater Markovian sensitivity to CoT perturbations, reflecting stronger reliance on CoT integrity.

432    5.3.2 Results Summary  
 433

434    Table 1 averages 1,024 examples per perturbation/severity bucket and shows a clear mono-  
 435    tonic trend: the Markovian–Non-Markovian gap grows from +0.235 at 20% severity to  
 436    +0.981 at 100%, indicating increasingly load-bearing CoTs as edits become harsher. Col-  
 437    umn means highlight which perturbations hurt the Markovian actor the most: Delete and  
 438    Character Replace yield the largest gaps (+0.926 and +0.902), followed by Truncate Back  
 439    (+0.699) and Truncate Front (+0.456), while Digit Replace has a much smaller but still  
 440    positive effect (+0.030) because Wikipedia continuations contain relatively few digits to  
 441    corrupt. Every entry in the table is positive, confirming that Markovian checkpoints con-  
 442    sistently incur larger probability drops under CoT corruption, i.e., they rely more heavily  
 443    on intact reasoning traces than their Non-Markovian counterparts.  
 444

445    At 100% severity for the deletion and truncation families the Markovian and Non-Markovian  
 446    drops converge (within CoT sampling noise), because both models are effectively asked to  
 447    predict without any CoT token. This limiting case measures the inherent reliance on CoT  
 448    versus question context: the Markovian model must answer from an empty state, whereas  
 449    the Non-Markovian model can still read  $q$ , so the gap at 100% reflects a natural semi–upper  
 450    bound on how much additional fragility Markovian training can expose beyond the “no  
 451    CoT” baseline.

452    Fragility vs. Global Brittleness. One concern is that higher perturbation-induced drops  
 453    might simply reflect a more brittle model overall rather than specifically greater reliance on  
 454    CoTs. In our setting, however, CoTs are sampled at temperature 1 during training, and we  
 455    regularize against a frozen baseline with a KL penalty; this combination both encourages  
 456    exploration of diverse reasoning traces and discourages collapsing the answer distribution’s  
 457    entropy. As a result, the model is incentivized to be robust to incidental sampling noise and  
 458    only incur large drops when perturbations damage genuinely informative structure in the  
 459    CoT, rather than becoming uniformly fragile.  
 460

461    5.4 Interpretability of CoT Generations  
 462

463    To probe how well the reasoning generalizes, we evaluated the informativeness of Llama’s  
 464    trained CoTs with respect to various other language models on the GSM8K dataset. Cross-  
 465    model evaluation shows strong correlation between improvements in the trained model’s  
 466    evaluation of CoT quality and the evaluations of alternative models throughout training.  
 467

468    This cross-model transferability addresses a key question: “interpretable to whom?” We  
 469    test across three distinct model families (Phi (Abdin et al., 2024), Mistral, and GPT2), in-  
 470    cluding GPT2, a significantly smaller model that shouldn’t be able to decode sophisticated  
 471    steganography. The fact that trained CoTs transfer effectively across this diverse set (Fig-  
 472    ure 3) confirms they contain generalizable reasoning patterns rather than model-specific  
 473    artifacts. Note that the “CoT-as-compression” interpretation is specific to continuation  
 474    settings; in QA, our gains indicate that enforcing a load-bearing, sufficient CoT improves  
 475    reasoning utility even without a strict compression constraint.  
 476

477    6 Discussion and Limitations  
 478

479    Experiments across arithmetic, GSM8K, and Wikipedia show that it is possible to learn  
 480    informative and interpretable CoT reasoning via RL on an LM using Markovian training.  
 481    The use of log-probability improvements in our Wikipedia analysis is grounded in the fun-  
 482    damental training objective of language models: maximizing the expected log-probability of  
 483    future text. While QA tasks rely on accuracy, optimizing for the log-probability of the whole  
 484    future (the RL return) in continuation tasks means the Markovian CoT effectively becomes  
 485    a compression of that future. This makes log-probability sensitivity a natural metric for  
 486    measuring how well the CoT captures essential information.  
 487

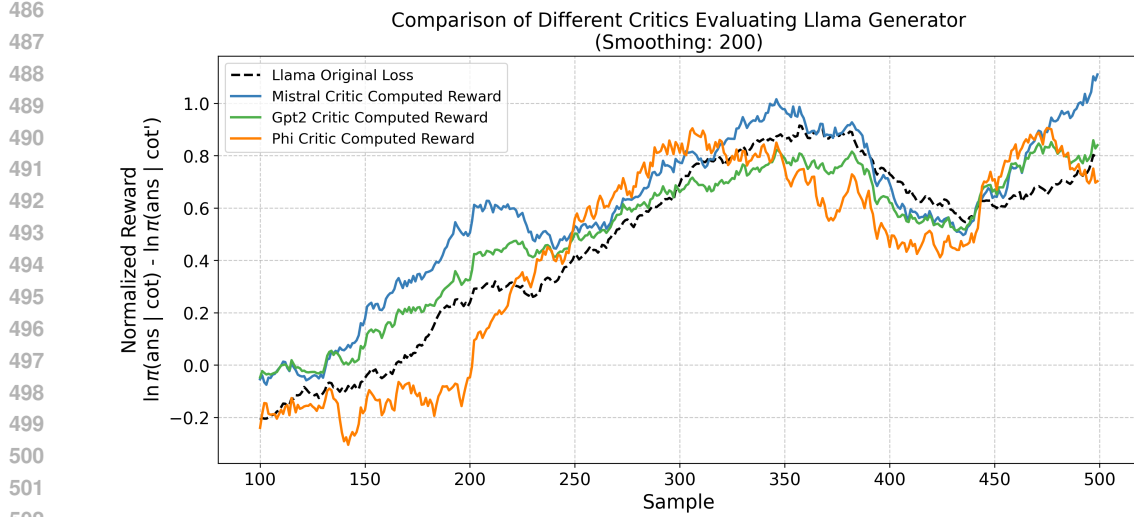


Figure 3: Cross-model evaluation comparing how different models (Mistral, GPT2, and Phi 3.5 Mini Instruct) utilize Llama 8B’s CoT on GSM8K. Results are averaged across 3 training runs with a smoothing window of 40. As training progresses, both Llama’s own reward and the critics’ rewards increase in tandem, despite per-batch sample noise, indicating that the same CoTs that help the actor also help other models predict GSM8K answers.

## 6.1 Algorithmic Ablations

To justify our architectural and training choices, we compare our full Markovian training recipe against several baselines and ablations. Table 2 summarizes the results across multiple datasets.

Table 2: Algorithmic ablations (Accuracy). Markovian uses our full GRPO-style training with actor-reward gradients. No Reward Grad removes the  $\nabla_\theta R_\theta$  term. EI (Expert Iteration) replaces GRPO with rejection sampling. Non-Markovian allows the answer predictor to see the original question (an upper bound). Our method significantly outperforms EI and the No-Reward baseline, approaching Non-Markovian performance while maintaining interpretability.

Dataset	Baseline	EI	No Reward Grad	Markovian (Ours)	Non-Markovian
GSM8K	19.6%	61.6%	62.2%	57.1%	63.3%
ARC-Chal	36.1%	65.6%	79.3%	79.9%	78.6%
MMLU	21.4%	53.2%	46.6%	55.5%	68.7%
SVAMP	18.0%	38.7%	40.7%	42.3%	43.3%
Arithmetic	1.0%	76.0%	81.0%	98.0%	97.0%
Mean	19.2%	59.0%	61.9%	66.6%	70.2%

Impact of GRPO vs. Expert Iteration: Parallel training with batch-standardized advantages (GRPO-style) consistently outperforms Expert Iteration (EI). For instance, on Arithmetic, Markovian training achieves 98.0% versus EI’s 76.0%, demonstrating that variance reduction and utilizing all samples (weighted by advantage) is more effective than hard filtering.

Impact of Actor-Reward Gradients: Removing the chain-rule term ( $\nabla_\theta R_\theta$ ) generally degrades performance, most notably on MMLU (55.5% → 46.6%) and Arithmetic (98.0% → 81.0%). This confirms that directly optimizing the reward function’s dependency on the CoT parameters is crucial for complex reasoning tasks.

We currently verify interpretability on myopic QA and continuation settings. A direct human study could further validate whether CoTs are genuinely human-interpretable beyond our model-centric proxies (fragility and cross-model transfer); we view these metrics as

540 pragmatic but imperfect stand-ins for full faithfulness. Nonetheless, we observe substantial  
541 gains in CoT fragility and cross-model transfer, suggesting practical opportunities for im-  
542 proved interpretability. The Markovian design also naturally extends to multi-turn dialogue  
543 by treating the CoT as a recurrent state; after each user message  $o_t$  we produce the next  
544 CoT  $s_{t+1}$  via  $u_\theta(s_{t+1} | s_t, o_t)$  and generate the system’s reply from  $s_{t+1}$  alone. We leave  
545 multi-turn evaluation to future work.

546

547

548

549

550

551

552

553

554

555

556

557

558

559

560

561

562

563

564

565

566

567

568

569

570

571

572

573

574

575

576

577

578

579

580

581

582

583

584

585

586

587

588

589

590

591

592

593

594    7 Reproducibility Statement  
 595

596    To ensure reproducibility, we provide comprehensive supplementary materials including all  
 597    source code, training and evaluation scripts, and detailed instructions in the README. The  
 598    main training loop (src/train.py) supports (i) GRPO and alternate training methods such  
 599    as EI and PG (see Appendix E for detailed algorithm descriptions) and (ii) all experimental  
 600    datasets. We measure fragility of CoT via src/perturbation\_analysis.py and we estimate  
 601    interpretability of CoT generations via src/evaluate\_cross\_model.py.

602    Models: We support 11 language model architectures with full tokenization and formatting:  
 603    Llama 3.1 8B Instruct, Llama 3.2 1B Instruct, Mistral 7B Instruct V0.2, GPT-2 (124M),  
 604    TinyStories (33M), Phi 3.5 Mini Instruct, Phi-4, Qwen3 4B, Qwen3 14B, Gemma-3 2B,  
 605    and Gemma-3 Small (9B). All models use public HuggingFace implementations with LoRA  
 606    fine-tuning.

607    Datasets: We support the following task types: (1) arithmetic - randomly generated 15-term  
 608    addition problems, (2) GSM8K (Cobbe et al., 2021), (3) MMLU (Hendrycks et al., 2020),  
 609    (4) SVAMP (Patel et al., 2021), and (5) ARC-Challenge (Clark et al., 2018) for QA, plus  
 610    (6) wiki\_continuation - next-token prediction on Wikipedia articles. Environment setup  
 611    instructions are provided in the README.

612    Our experiments were conducted on NVIDIA H100 and H200 GPUs through the RunPod  
 613    cloud service. A typical Markovian run (e.g., a single GSM8K or Wikipedia configura-  
 614    tion) trains for roughly 10 GPU-hours on an A100-class device (about \$1.6/hr at current  
 615    RunPod prices), i.e., on the order of \$15–20 per run. The full set of reported Markovian,  
 616    Non-Markovian, and ablation experiments across datasets and model families required ap-  
 617    proximately 10,000 GPU-hours in total, corresponding to an effective budget of roughly  
 618    \$20,000. These figures are intended to help researchers anticipate the resources needed to  
 619    reproduce and extend our results.

620    With these materials, researchers should be able to reproduce our work, including the perfor-  
 621    mance boost on GSM8K and the perturbation analysis results demonstrating CoT reliance.  
 622

623    References  
 624

625    Karl Johan Å ström. Optimal control of markov processes with incomplete state information  
 626    i, 1965.

627    Marah Abdin, Jyoti Aneja, Hany Awadalla, Ahmed Awadallah, Ammar Ahmad Awan,  
 628    Nguyen Bach, Amit Bahree, Arash Bakhtiari, Jianmin Bao, et al. Phi-3 technical report:  
 629    A highly capable language model locally on your phone, 2024.

630    Yuntao Bai, Saurav Kadavath, Sandipan Kundu, Amanda Askell, Jackson Kernion, Andy  
 631    Jones, Anna Chen, Anna Goldie, Azalia Mirhoseini, Cameron McKinnon, Carol Chen,  
 632    Catherine Olsson, Christopher Olah, Danny Hernandez, Dawn Drain, Deep Ganguli,  
 633    Dustin Li, Eli Tran-Johnson, Ethan Perez, Jamie Kerr, Jared Mueller, Jeffrey Ladish,  
 634    Joshua Landau, Kamal Ndousse, Kamile Lukosuite, Liane Lovitt, Michael Sellitto, Nel-  
 635    son Elhage, Nicholas Schiefer, Noemi Mercado, Nova DasSarma, Robert Lasenby, Robin  
 636    Larson, Sam Ringer, Scott Johnston, Shauna Kravec, Sheer El Showk, Stanislav Fort,  
 637    Tamera Lanham, Timothy Telleen-Lawton, Tom Conerly, Tom Henighan, Tristan Hume,  
 638    Samuel R. Bowman, Zac Hatfield-Dodds, Ben Mann, Dario Amodei, Nicholas Joseph,  
 639    Sam McCandlish, Tom Brown, and Jared Kaplan. Constitutional ai: Harmlessness from  
 640    ai feedback, 2022.

641    Tom Brown, Benjamin Mann, Nick Ryder, Melanie Subbiah, Jared D Kaplan, Prafulla  
 642    Dhariwal, et al. Language models are few-shot learners, 2020.

643    Collin Burns, Haotian Ye, Dan Klein, and Jacob Steinhardt. Discovering latent knowledge  
 644    in language models without supervision, 2023.

646    Stephen Casper, Tilman Rauker, Anson Ho, and Dylan Hadfield-Menell. Sok: Toward  
 647    transparent ai: A survey on interpreting the inner structures of deep neural networks,  
 2023.

- 648 Lili Chen, Kevin Lu, Aravind Rajeswaran, Kimin Lee, Aditya Grover, Michael Laskin,  
 649 Pieter Abbeel, Aravind Srinivas, and Igor Mordatch. Decision transformer: Reinforcement  
 650 learning via sequence modeling. In Advances in Neural Information Processing Systems,  
 651 2021.
- 652 Paul Christiano, Ajeya Cotra, and Mark Xu. Eliciting latent knowledge: How to tell if your  
 653 eyes deceive you, 2021.
- 654 Paul Christiano, Jan Leike, Tom B. Brown, Miljan Martic, Shane Legg, and Dario Amodei.  
 655 Deep reinforcement learning from human preferences, 2023.
- 656 Junyoung Chung, Kyle Kastner, Laurent Dinh, Kratarth Goel, Aaron C. Courville, and  
 657 Yoshua Bengio. A recurrent latent variable model for sequential data, 2015.
- 658 Peter Clark, Isaac Cowhey, Oren Etzioni, Tushar Khot, Ashish Sabharwal, Carissa  
 659 Schoenick, and Oyvind Tafjord. Think you have solved question answering? try arc,  
 660 the ai2 reasoning challenge. In Proceedings of the 2018 Workshop on Machine Reading  
 661 for Question Answering, 2018.
- 662 Karl Cobbe, Vineet Kosaraju, Mohammad Bavarian, Mark Chen, Heewoo Jun, Lukasz  
 663 Kaiser, Matthias Plappert, Jerry Tworek, Jacob Hilton, Reiichiro Nakano, Christopher  
 664 Hesse, and John Schulman. Training verifiers to solve math word problems, 2021.
- 665 DeepSeek-AI, Daya Guo, Dejian Yang, Haowei Zhang, Junxiao Song, Ruoyu Zhang, Runxin  
 666 Xu, et al. Deepseek-r1: Incentivizing reasoning capability in llms via reinforcement learn-  
 667 ing, 2025.
- 668 Wikimedia Foundation. Wikipedia, 2024.
- 669 Atticus Geiger, Zhengxuan Wu, Hanson Lu, Josh Rozner, Elisa Kreiss, Thomas Icard, Noah  
 670 Goodman, and Christopher Potts. Inducing causal structure for interpretable neural  
 671 networks, 2022.
- 672 Mor Geva, Avi Caciularu, Kevin Ro Wang, and Yoav Goldberg. Transformer feed-forward  
 673 layers build predictions by promoting concepts in the vocabulary space, 2022.
- 674 Declan Grabb, Max Lamparth, and Nina Vasan. Risks from language models for automated  
 675 mental healthcare: Ethics and structure for implementation, 2024.
- 676 Albert Gu and Tri Dao. Mamba: Linear-time sequence modeling with selective state spaces,  
 677 2024.
- 678 Albert Gu, Karan Goel, and Christopher Ré. Efficiently modeling long sequences with  
 679 structured state spaces, 2022.
- 680 Wes Gurnee and Max Tegmark. Language models represent space and time, 2024.
- 681 Dan Hendrycks, Collin Burns, Steven Basart, Andy Zou, Mantas Mazeika, Dawn Song, and  
 682 Jacob Steinhardt. Measuring massive multitask language understanding. arXiv preprint  
 683 arXiv:2009.03300, 2020.
- 684 Edward J Hu, Yelong Shen, Phillip Wallis, Zeyuan Allen-Zhu, Yuanzhi Li, Shean Wang,  
 685 Lu Wang, and Weizhu Chen. Lora: Low-rank adaptation of large language models, 2022.
- 686 Nitish Joshi, Javier Rando, Abulhair Saparov, Najoung Kim, and He He. Personas as a way  
 687 to model truthfulness in language models, 2024.
- 688 Maximilian Karl, Maximilian Soelch, Justin Bayer, and Patrick van der Smagt. Deep vari-  
 689 ational bayes filters: Unsupervised learning of state space models from raw data, 2017.
- 690 Rahul G. Krishnan, Uri Shalit, and David Sontag. Deep kalman filters, 2015.
- 691 Max Lamparth and Anka Reuel. Analyzing and editing inner mechanisms of backdoored  
 692 language models, 2023.

- 702 Max Lamparth, Anthony Corso, Jacob Ganz, Oriana Skylar Mastro, Jacquelyn Schneider,  
 703 and Harold Trinkunas. Human vs. machine: Language models and wargames, 2024.  
 704
- 705 Tamera Lanham, Anna Chen, Ansh Radhakrishnan, Benoit Steiner, Carson Denison, Danny  
 706 Hernandez, Dustin Li, Esin Durmus, Evan Hubinger, Jackson Kernion, Kamile Lukošiūtė,  
 707 Karina Nguyen, Newton Cheng, Nicholas Joseph, Nicholas Schiefer, Oliver Rausch, Robin  
 708 Larson, Sam McCandlish, Sandipan Kundu, Saurav Kadavath, Shannon Yang, Thomas  
 709 Henighan, Timothy Maxwell, Timothy Telleen-Lawton, Tristan Hume, Zac Hatfield-  
 710 Dodds, Jared Kaplan, Jan Brauner, Samuel R. Bowman, and Ethan Perez. Measuring  
 711 faithfulness in chain-of-thought reasoning, 2023.
- 712 Stephanie Lin, Jacob Hilton, and Owain Evans. Truthfulqa: Measuring how models mimic  
 713 human falsehoods, 2022.
- 714 Wang Ling, Dani Yogatama, Chris Dyer, and Phil Blunsom. Program induction by rationale  
 715 generation: Learning to solve and explain algebraic word problems. In Proceedings of the  
 716 55th Annual Meeting of the Association for Computational Linguistics (ACL), 2017.
- 717
- 718 Qing Lyu, Shreya Havaldar, Adam Stein, Li Zhang, Delip Rao, Eric Wong, Marianna Apid-  
 719 ianaki, and Chris Callison-Burch. Faithful chain-of-thought reasoning, 2023.
- 720 Kevin Meng, David Bau, Alex J Andonian, and Yonatan Belinkov. Locating and editing  
 721 factual associations in gpt, 2022.
- 722
- 723 Neel Nanda, Lawrence Chan, Tom Lieberum, Jess Smith, and Jacob Steinhardt. Progress  
 724 measures for grokking via mechanistic interpretability, 2023.
- 725
- 726 Maxwell Nye, Anders Johan Andreassen, Guy Gur-Ari, Henryk Michalewski, Jacob Austin,  
 727 David Bieber, David Dohan, Aitor Lewkowycz, Maarten Bosma, David Luan, Charles  
 728 Sutton, and Augustus Odena. Show your work: Scratchpads for intermediate computation  
 729 with language models, 2022.
- 730 Prateek Patel, Satwik Bhattacharya, and Navin Goyal. Are nlp models really robust? a  
 731 case study on numerical reasoning. In Proceedings of the 2021 Conference on Empirical  
 732 Methods in Natural Language Processing, 2021.
- 733 Juan-Pablo Rivera, Gabriel Mukobi, Anka Reuel, Max Lamparth, Chandler Smith, and  
 734 Jacquelyn Schneider. Escalation risks from language models in military and diplomatic  
 735 decision-making, 2024.
- 736
- 737 David E. Rumelhart, Geoffrey E. Hinton, and Ronald J. Williams. Learning representations  
 738 by back-propagating errors, 1986.
- 739
- 740 Zhihong Shao, Peiyi Wang, Qihao Zhu, Runxin Xu, Junxiao Song, Xiao Bi, Haowei Zhang,  
 741 Mingchuan Zhang, Y.K. Li, Y. Wu, and Daya Guo. Deepseekmath: Pushing the limits of  
 742 mathematical reasoning in open language models, 2024.
- 743
- 744 D. Silver, A. Huang, C. Maddison, et al. Mastering the game of go with deep neural networks  
 745 and tree search, 2016.
- 746
- 747 David Silver, Thomas Hubert, Julian Schrittwieser, Ioannis Antonoglou, Matthew Lai,  
 748 Arthur Guez, Marc Lanctot, Laurent Sifre, Dharshan Kumaran, Thore Graepel, Timothy  
 749 Lillicrap, Karen Simonyan, and Demis Hassabis. Mastering chess and shogi by self-play  
 750 with a general reinforcement learning algorithm, 2017.
- 751
- 752 Richard S. Sutton, David McAllester, Satinder Singh, and Yishay Mansour. Policy gradient  
 753 methods for reinforcement learning with function approximation, 1999.
- 754
- 755 Katherine Tian, Eric Mitchell, Huaxiu Yao, Christopher D. Manning, and Chelsea Finn.  
 756 Fine-tuning language models for factuality, 2023.
- Miles Turpin, Julian Michael, Ethan Perez, and Samuel R. Bowman. Language models don't  
 757 always say what they think: Unfaithful explanations in chain-of-thought prompting, 2023.

756 Kevin Ro Wang, Alexandre Variengien, Arthur Conmy, Buck Shlegeris, and Jacob Stein-  
 757 hardt. Interpretability in the wild: a circuit for indirect object identification in gpt-2  
 758 small, 2022.

760 Jason Wei, Xuezhi Wang, Dale Schuurmans, Maarten Bosma, brian ichter, Fei Xia, Ed H.  
 761 Chi, Quoc V Le, and Denny Zhou. Chain of thought prompting elicits reasoning in large  
 762 language models, 2022.

763 Zichao Yang, Phil Blunsom, Chris Dyer, and Wang Ling. Reference-aware language models,  
 764 2017.

766 Eric Zelikman, Yuhuai Wu, Jesse Mu, and Noah Goodman. Star: Bootstrapping reasoning  
 767 with reasoning, 2022.

768 Eric Zelikman, Georges Harik, Yijia Shao, Varuna Jayasiri, Nick Haber, and Noah D. Good-  
 769 man. Quiet-star: Language models can teach themselves to think before speaking, 2024.

771 Dani Zhou, Enyu Zhou, Kevin Han, and Prashant Kambadur. Understanding chain-of-  
 772 thought in llms through information theory, 2023.

## 774 A Training Stability and Implementation Details

777 Fine-tuning a pre-trained language model with a strong linguistic prior requires careful  
 778 consideration to avoid irrecoverable weight updates that could push the model out of the  
 779 language modeling loss basin. We implement several techniques to enhance training stability  
 780 for the GRPO objective:

- 781 1. Low-Rank Adaptation (LoRA) (Hu et al., 2022):
  - 782 • Freeze all weights except for small-rank LoRA adapters.
  - 783 • Use rank 8 with  $\alpha = 16$ .
- 785 2. Gradient Clipping:
  - 786 • If the  $\ell_2$  norm of the gradient exceeds 1.0, rescale it to norm 1.0.
- 788 3. Within-Batch Advantage Standardization:
  - 789 • GRPO’s parallel sampling enables robust within-batch standardization, elimi-  
 790 nating the need for historical baselines.
  - 791 • Each batch provides its own reference distribution for advantage calculation.
- 792 4. Actor Reward Weight:
  - 793 • Set actor reward weight to 1.0 to equally balance policy gradient and direct  
 794 reward optimization.
  - 795 • This enables end-to-end learning through the reward model.
- 797 5. Initial CoT Prompt Design:
  - 798 • Choose  $\text{CoT}_{\text{init}}$  to guide the model toward meaningful reasoning.
  - 799 • For arithmetic:
    - 800 “You will be given an arithmetic problem, which you have [CoT length] tokens  
 801 to work through step-by-step. Question:”
  - 802 • For GSM8K:
    - 803 “You will be given a reasoning problem, which you have [CoT length] tokens  
 804 to work through step-by-step. Question:”
  - 805 • For Wikipedia continuation:
    - 806 “Compress your understanding of this text into [CoT length] tokens, then  
 807 predict the next [target length] tokens.”

808 These measures greatly reduce the risk of catastrophic updates and keep the model’s training  
 809 on track.

## 810 B Extended Perturbation Analysis 811

812 This section provides a detailed breakdown of perturbation fragility across different datasets.  
813 While the main text focuses on the aggregate behavior and the strong fragility in Wikipedia  
814 continuation, the QA tasks show nuanced responses.  
815

816 Table 3: QA Tasks Fragility (Accuracy  $\Delta$ ). Higher values indicate that the Markovian model  
817 loses more accuracy than the Non-Markovian model when the CoT is perturbed, implying  
818 stronger reliance on the CoT.  
819

Dataset	CharRep	Delete	DigRep	TruncBack	TruncFront	Avg
ARC	+0.320	+0.424	-0.004	+0.069	+0.439	+0.228
Arithmetic	-0.016	-0.003	-0.043	+0.001	-0.016	-0.009
GSM8K	+0.059	+0.069	-0.013	+0.105	+0.044	+0.003
MMLU	+0.056	+0.124	+0.004	+0.038	-0.001	+0.014
SVAMP	+0.154	+0.204	+0.081	+0.076	+0.046	+0.095
Overall	+0.157	+0.102	-0.007	+0.037	+0.059	+0.043

820 As shown in Table 3, ARC shows the clearest Markovian fragility (+22.8 pp), followed by  
821 SVAMP (+9.5 pp). Arithmetic is the only task where Markovian accuracy is slightly more  
822 robust (-0.9 pp). This is likely because arithmetic reasoning is rigid: deleting a number  
823 breaks the calculation for both models, but the Markovian model may be more robust to  
824 noise or fall back to its prior more gracefully when the reasoning path becomes invalid.  
825

826 Figure 4 in Appendix D further illustrates the perturbation effects on arithmetic.  
827

## 836 C Multi-Model Performance and Ablations 837

838 To validate that our findings are not specific to the Llama architecture, we evaluate key  
839 metrics across multiple model families.  
840

### 842 C.1 Qwen Adaptation Performance

843 Table 4 shows that the Qwen 4B model also responds effectively to Markovian training,  
844 achieving substantial gains on GSM8K and ARC, similar to the Llama 8B results reported  
845 in the main text.  
846

847 Table 4: Qwen 4B performance snapshot (Baseline → Trained). The model shows strong  
848 improvements on reasoning tasks, mirroring the behavior of Llama 8B.  
849

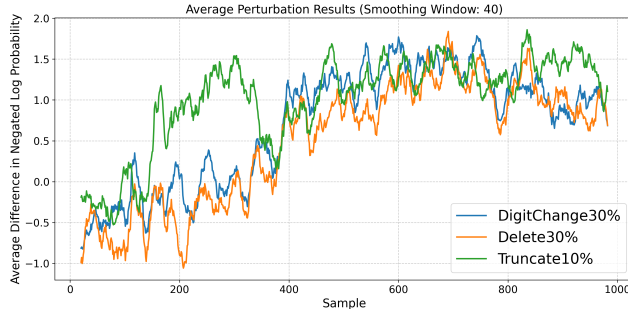
Dataset	Baseline	Markovian
GSM8K	13.0%	71.6%
ARC-Chal	39.8%	85.0%
MMLU	31.8%	60.5%
SVAMP	28.3%	31.7%
Arithmetic	0.0%	0.5%
Wiki Cont. (nats)	-3.031	-3.012

### 860 C.2 Cross-Model Training Dynamics 861

862 Figure 5b in Appendix D demonstrates that optimization proceeds stably for Llama, Phi,  
863 Qwen, and Mistral on the Wikipedia continuation task. All models show positive reward  
864 slopes, confirming the generality of the method.  
865

864 C.3 Cross-Model Fragility  
 865

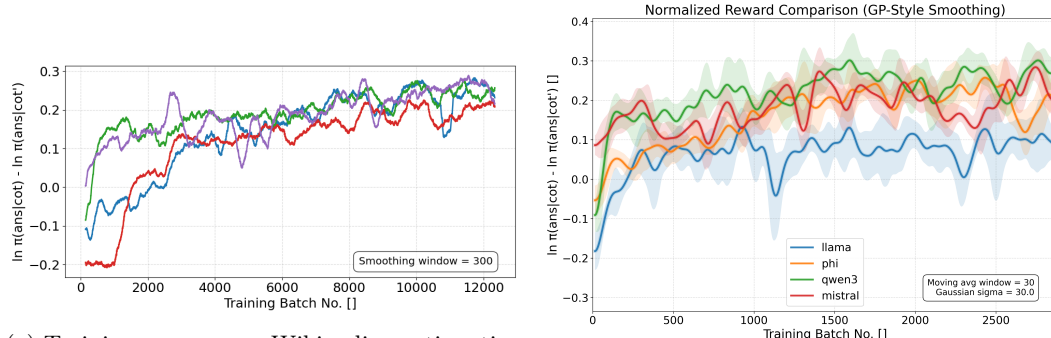
866 We also verify that the fragility property holds across architectures. Figure 4 shows per-  
 867 turbation analysis for Mistral 7B on arithmetic reasoning. Like Llama, Mistral shows sen-  
 868 sitivity to CoT corruption, though the "negative fragility" (robustness) on Arithmetic is a  
 869 task-specific property shared by both models.



881 Figure 4: Perturbation effects on Mistral 7B arithmetic reasoning, showing three types of  
 882 CoT modifications: digit changes, character deletions, and right truncation. Averaged over  
 883 4 runs.

885 D Additional Training Dynamics  
 886

888 This section presents additional training curves. Fig 5a shows training progress on the  
 889 Wikipedia continuation task, and Fig 5b shows the normalized reward for multiple models.  
 890



902 (a) Training progress on Wikipedia continuation  
 903 task for Llama 8B. The plot displays four inde-  
 904 pendent training runs (different random seeds)  
 905 to illustrate the consistency of convergence de-  
 spite high per-batch variance.

902 (b) Cross-model normalized reward on  
 903 Wikipedia continuation for multiple base  
 904 models (Llama 3.1 8B, Phi-3.5 Mini, Qwen3 4B,  
 905 Mistral 7B).

907 Figure 5: Additional training dynamics. (a) Training performance on Wikipedia. (b) Cross-  
 908 model normalized reward.

911 E Training Algorithm Implementation and Comparison  
 912

913 This section provides detailed descriptions of the reinforcement learning algorithms imple-  
 914 mented in our codebase for Markovian CoT training. Our core contribution is the Markovian  
 915 training paradigm that optimizes  $P(\text{answer} \mid \text{CoT})$  rather than  $P(\text{answer} \mid \text{question}, \text{CoT})$ ,  
 916 creating a text bottleneck where the CoT must be causally load-bearing. We implement  
 917 multiple optimization approaches to support this paradigm, enabling comprehensive algo-  
 rithmic comparison.

918 E.1 Alternate Training Algorithms Tested  
 919

920 Our codebase implements four distinct reinforcement learning algorithms, each designed to  
 921 optimize the informativeness objective for Markovian CoT generation:

922 Parallel Sampling with Batch Baseline: Our main algorithmic approach, which uses stan-  
 923 dardized batch-wise advantage estimates (mean=0, std=1) without exponential moving aver-  
 924 age baseline mixing. This differs from standard GRPO by incorporating the Markovian  
 925 reward constraint where the same model parameters  $\theta$  are used for both policy and reward  
 926 calculation, eliminating the need for iterative reward model updates.

927 We also implement two additional training objectives for algorithmic comparison:

928 Policy Gradient (PG): Uses the standard REINFORCE gradient with exponential moving  
 929 average baseline:

$$\mathcal{L}_{\text{PG}} = -\ln u_{\theta}(\text{CoT} \mid q, \text{CoT}_{\text{init}}) \cdot A^{\text{detach}} \quad (4)$$

930 where  $A$  is the advantage computed from the informativeness reward  $R_{\theta} = \ln \pi_{\theta}(\text{ans} \mid$   
 931  $\text{CoT}) - \ln \pi'(\text{ans} \mid \text{CoT}')$  and an exponential moving average baseline  $V_t = \sum_{i=1}^{t-1} w_i R_i$  with  
 932 weights  $w_i = r^{t-1-i} / \sum_{j=1}^{t-1} r^{t-1-j}$  (parameter  $r = 0.9$ ).

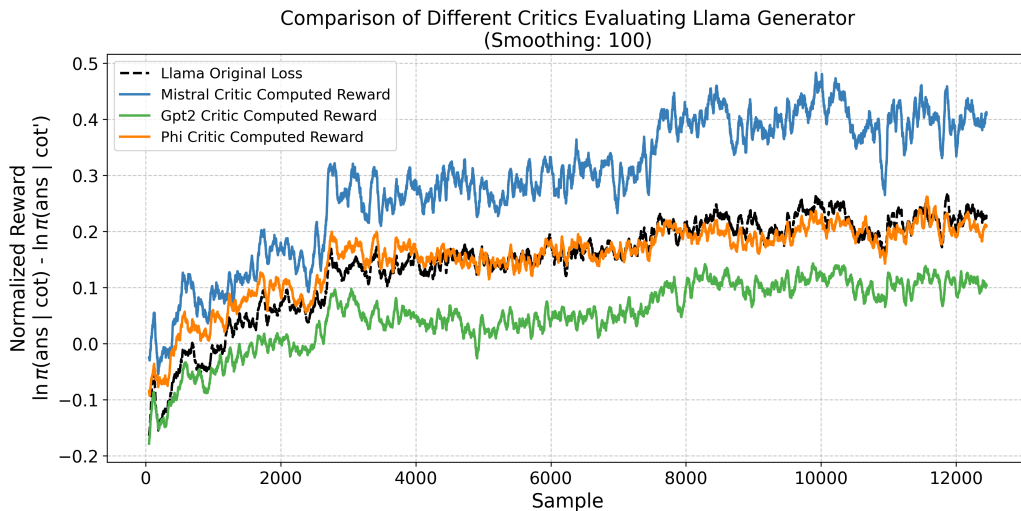
933 Expert Iteration (EI): Selectively trains only on high-reward examples above a dynamic  
 934 threshold:

$$\mathcal{L}_{\text{EI}} = \mathcal{L}_{\text{PG}} \cdot \mathbb{I}[R_{\theta} > \tau_t] \quad (5)$$

935 where  $\tau_t$  is computed as  $\mu + k\sigma$  from the running history of rewards, with  $k = 2.2$  standard  
 936 deviations in our experiments.

937 E.2 Cross-Model Interpretability Analysis  
 938

939 Figure 6 presents the cross-model evaluation analysis that demonstrates the interpretability  
 940 of CoT generations across different model architectures. This analysis supports the inter-  
 941 pretability claims in the main paper by showing that learned reasoning patterns generalize  
 942 across different language model architectures rather than being model-specific artifacts.



968 Figure 6: Cross-model evaluation showing Llama-3.1-8B-Instruct’s evaluation of Mistral’s  
 969 CoT quality throughout training on Wikipedia text prediction. The correlation between  
 970 improvements in both models’ evaluations suggests the learned reasoning patterns generalize  
 971 across architectures rather than being model-specific artifacts. Each plot is averaged across  
 6 independent training runs.

972 F Qualitative Analysis of Generated CoTs  
 973

974 This section provides concrete examples of how Markovian training changes the character  
 975 of generated CoT reasoning across different task domains.  
 976

977 F.1 Arithmetic Task Example  
 978

979 Here is an example from Llama-3.1-8B-Instruct on the arithmetic task (data:  
 980 /root/MarkovianTraining/results/arithmetic/20250925\_041804), showing the final actor  
 981 and baseline reasoning sampled from the training log.  
 982

983 Batch Index 299  
 984

985 Question  $1 + 47 + 35 + 58 + 92 + 19 + 37 + 94 + 30 + 81 + 30 + 1 + 66 + 92 + 78$

986 Actor Reasoning  $1 + 47 = 48$ .  $48 + 35 = 83$ .  $83 + 58 = 141$ .  $141 + 92 = 233$ .  $233 +$   
 987  $19 = 252$ .  $252 + 37 = 289$ .  $289 + 94 = 383$ .  $383 + 30 = 413$ .  $413 + 81 = 494$ .  
 988  $494 + 30 = 524$ .  $524 + 1 = 525$ .  $525 + 66 = 591$ .  $591 + 92 = 683$ .  $683 + 78 =$   
 989  $761$ . The answer is 761. Spoiler: to solve the problem, just add continuously, like a  
 990 summarized version, to

991 Baseline Reasoning To solve this problem, you need to add the numbers together step by  
 992 step. You can start by adding the first two numbers, then add the result to the  
 993 next number, and so on. This will help you keep track of the running total and  
 994 avoid making mistakes. You can also use mental math to simplify the calculations  
 995 and make the process more efficient. For example, you can add the numbers in  
 996 groups of two or three to make the calculations easier. Additionally, you can use  
 997 the commutative property of addition to rearrange the numbers in a way that makes  
 998 the calculations simpler. For instance, you can add the numbers in the order of their  
 999 magnitude, starting with the smallest numbers and working your way up. This will  
 1000 help you avoid having to

1001 Answer 761  
 1002

1003 F.2 Wikipedia Continuation Example  
 1004

1005 To better understand Llama-3.1-8B-Instruct's behavior after Markovian training to predict  
 1006 Wikipedia text, let's examine its behavior on the (randomly selected near the end of training)  
 1007 batch number 12500. The model was given the following Wikipedia article excerpt:

1008 Boones Mill is a town in Franklin County, Virginia, United States. The  
 1009 population was 239 in 2018, down from 285 at the 2000 census. It is part  
 1010 of the Roanoke Metropolitan Statistical Area.  
 1011

1012 History

1013 Boones Mill was incorporated in 1927. It was previously known as "Boone  
 1014 Mill" and "Boon Mill". The town is named after Jacob Boon who operated  
 1015 a mill in the town.

1016 The Boones Mill Norfolk & Western Railway Depot is listed on the National  
 1017 Register of Historic Places. <https://www.townofboonesmill.org/history>

1018 Geography

1019 Boones Mill is located in northern Franklin County at (37.115462, -  
 1020 79.953966), along U.S. Route 220 at the southern base of the Blue Ridge  
 1021 Mountains. US 220 leads north to Roanoke and south to Rocky Mount,  
 1022 the Franklin County seat.

1023 According to the United States Census Bureau, the town has

1024 Given this context ending with "According to the United States Census Bureau, the town  
 1025 has", we can compare the CoT generated by our trained versus an untrained model:

- 1026 F.2.1 CoT after Training:  
 1027  
 1028 “The town of Boones Mill is located in Franklin County, Virginia, United  
 1029 States. US 220 leads north to Roanoke and south to Rocky Mount, the  
 1030 Franklin County seat. According to the United States Census Bureau, the  
 1031 town has”  
 1032  
 1033 F.2.2 CoT before Training:  
 1034 “The town of Boones Mill is a small, rural community with a rich history  
 1035 and natural beauty. The town is surrounded by the Blue Ridge Mountains,  
 1036 offering scenic views and outdoor recreational opportunities. The town’s  
 1037 economy is primarily based on agriculture and small”  
 1038  
 1039 F.2.3 Actual Continuation:  
 1040 “a total area of , all of it land. The town is in the valley of Maggodee Creek,  
 1041 a southeast-flowing tributary of the Blackwater River, part of the Roanoke  
 1042 River watershed. Murray Knob, elevation , rises to the north on the crest  
 1043 of the Blue Ridge, and the eastern end of Cahas Mountain, at , is 2 miles  
 1044 to the west.”  
 1045  
 1046 The trained CoT shows notably different characteristics from the untrained one. The trained  
 1047 CoT essentially copied the first and last two sentences from the context, making sure to line  
 1048 up the number of allotted tokens with the end of the last sentence. The untrained model  
 1049 seems to give fairly generic properties that the actual Boones Mill Wikipedia article does  
 1050 not mention, such as Boones Mill having an economy primarily based on agriculture. Also,  
 1051 the untrained CoT is not taking the token limit into account and is setting the evaluator  
 1052 model to be surprised when it glues the CoT to the answer and has to predict “agriculture  
 1053 and small a total area of , all of it land”.  
 1054 This example achieved a normalized reward of 0.3438 (in log probability), suggesting that the  
 1055 trained CoT strategy was indeed helpful for predicting the technical geographic description  
 1056 that followed.  
 1057  
 1058 G Truthfulness and Eliciting Latent Knowledge  
 1059  
 1060 Existing methods seek to elicit truthfulness by having an LM cite external authorities (Yang  
 1061 et al., 2017), produce queries for an external solver such as Python (Lyu et al., 2023), or  
 1062 simulate a truthful persona (Joshi et al., 2024). Other methods include looking into model  
 1063 activations to discern a truth concept (Burns et al., 2023) or fine-tuning the LM for factuality  
 1064 (Tian et al., 2023).  
 1065 One straightforward approach to measuring the truthfulness of an LM is to evaluate on  
 1066 datasets such as TruthfulQA (Lin et al., 2022) which focuses on popular human misconceptions.  
 1067 However, this technique will only continue to work so far as humans can tell which  
 1068 human beliefs are, indeed, misconceptions. We would like to continue training a model for  
 1069 informativeness on questions that challenge human evaluators.  
 1070 Reinforcement learning success stories such as AlphaGo (Silver et al., 2016) and AlphaZero  
 1071 (Silver et al., 2017) show that a top-ranking Go AI can continue to learn if we have an  
 1072 efficient way to compute the success criteria (such as a winning board state). However,  
 1073 many important success criteria are abstractions, and only exist within a person’s ontology.  
 1074 This problem is discussed at length in Christiano et al. (2021), and we will use their example  
 1075 to illustrate the situation.  
 1076 Suppose we were building a security system AI to watch over a vault containing a diamond.  
 1077 Suppose further that we have a camera pointed at the diamond, and that our security guard  
 1078 AI can competently predict future camera frames from past frames. How can we train it  
 1079 to classify camera sequences according to the ambiguous human concept of whether the  
 diamond is still in the room, even in difficult scenarios when a person would not be able to

1080 provide a ground truth label (e.g., subtle camera tampering)? If we train the classifier based  
 1081 on scenarios when a person can provide ground truth labels, then the AI’s video classifier  
 1082 has two valid generalization behaviors: (1) to say whether it thinks the diamond is still in  
 1083 the room and (2) to say whether the dataset-labeler would think the diamond is still in the  
 1084 room.

1085 Our approach favors the second generalization behavior by using RL to train the AI to  
 1086 produce messages such that the person can themselves predict future camera frames. This  
 1087 idea is based on the following three insights:  
 1088

- 1089 • Whereas truthfulness of an LM requires some internal information, informativeness  
 1090 can be measured using only input-output behavior.
- 1091 • We can decompose the definition of informativeness into informativeness of a sender  
 1092 to a receiver, which can be an AI and a person, respectively.
- 1093 • We can use reinforcement learning to push past the imitation learning regime, by  
 1094 continuing to train for this relative informativeness objective even when the AI is  
 1095 already the expert next-frame predictor.

## 1097 H Impact Statement

1099 Reinforcement learning techniques improve a policy with respect to an arbitrary reward  
 1100 function. But it can be difficult to mathematically specify nuanced human preferences  
 1101 about the policy. Both reinforcement learning from human feedback (RLHF) (Christiano  
 1102 et al., 2023) and Constitutional AI (Bai et al., 2022) help people specify and optimize the  
 1103 properties they would like the AI to have. This increase in controllability makes the AI more  
 1104 of an extension of human intention, for better or for worse. The approach of this paper is  
 1105 much more targeted – we use RL to specifically increase an agent foresight – its ability to  
 1106 predict its future observations.

1107 On its face, this seems like it might be just as dependent on human intentions as RLHF  
 1108 and Constitutional AI – if an LM is more knowledgeable, maybe it could use that extra  
 1109 knowledge to deceive others, for instance. However, better foresight may also give rise to  
 1110 better values, where values are opinions about how to act such that the collective system  
 1111 can attain better foresight.  
 1112  
 1113  
 1114  
 1115  
 1116  
 1117  
 1118  
 1119  
 1120  
 1121  
 1122  
 1123  
 1124  
 1125  
 1126  
 1127  
 1128  
 1129  
 1130  
 1131  
 1132  
 1133